

## Chapter 3

### Structure-Based Drug Design Targeting Glutathione Synthetase of *Leishmania donovani* \*

#### Abstract

The current chapter focuses on identifying new anti-leishmanial compounds targeting the glutathione synthetase enzyme of the parasite. To achieve this, we conducted a drug repurposing approach extensively screening inhibitors from the FDA-approved ZINC database against *Leishmania donovani* glutathione synthetase by computational methods. First, the three-dimensional structure of *Leishmania donovani* glutathione synthetase was constructed by homology modeling, using the crystallographic structure of *Trypanosoma brucei* glutathione synthetase as a template. Subsequently, molecular docking studies were carried out for a large number of compounds using AutoDock Vina. Among the screened compounds, the top five compounds with strong binding affinity to *Leishmania donovani* glutathione synthetase but having a very low affinity to its human homolog were selected. Further investigations on protein-ligand complexes were carried out by conducting molecular dynamics (MD) simulation and MM/PBSA analysis. These findings showed that these compounds have the potential to act as inhibitors of glutathione synthetase. Hence, our study provides valuable insights for the development of a novel therapeutic strategy against *Leishmania donovani* by targeting the glutathione synthetase enzyme.

---

\* Part of the work is published in Sarma, M., Borkotoky, S., & Dubey, V.K\*. (2024) Structure-based drug designing against *Leishmania donovani* using docking and molecular dynamics simulation studies: exploring glutathione synthetase as a drug target. Journal of biomolecular structure & dynamics, 42(14), 7628–7636.

### 3.1 Introduction

Leishmaniasis is a vector-borne broad spectrum of clinical manifestations caused by various species of *Leishmania* parasite. More than 90 different species of sandflies of the genus *Phlebotomus* act as vectors for Leishmaniasis. The disease is categorized into three primary forms: visceral, cutaneous, and mucocutaneous. The visceral form is the most severe and common in India, caused by *Leishmania donovani* and *Leishmania infantum*. The majority of cases of visceral leishmaniasis (VL) are reported in India, Brazil, and East Africa. Globally, an estimated 50,000–90,000 new cases of visceral leishmaniasis occur each year, with only 25 to 45% being reported (World Health Organization, 2025).

The current treatment regime for Leishmaniasis have a limited number of chemotherapeutic drugs, including pentavalent antimonials miltefosine, amphotericin B, and Paromomycin sulfate. However, these drugs have different limitations such as severe side effects, drug resistance, low efficacy, and high treatment costs (Tiwari et al., 2017).

Furthermore, the development of an effective vaccine against Leishmaniasis is still a challenge. Notably, VL/HIV coinfection causes a significant threat to the control of visceral leishmaniasis (World Health Organization, 2025). Therefore, there is an urgent requirement of identifying novel drug targets as well as developing effective and affordable drug candidates against the parasite. In the rational drug discovery process, the identification and characterization of an enzyme or pathway as a suitable drug target in the parasite is a crucial step. The selected target should either be absent or significantly different from its human host. One such pathway is the trypanothione-based redox metabolism found in *Leishmania* and other trypanosomatids. This pathway has been extensively studied and identified as a unique mechanism for

neutralizing reactive oxygen species (ROS) generated within macrophages (Chawla & Madhubala, 2010; Colotti et al., 2013). Glutathione synthetase, an enzyme in this pathway, catalyzes a crucial step: the ATP-dependent formation of glutathione (GSH) from c-glutamylcysteine (c-GC) and L-glycine. Another reaction in the pathway involves the synthesis of spermidine from putrescine by ornithine decarboxylase and spermidine synthase. Glutathione is then coupled with spermidine via glutathionyl spermidine synthetase, resulting in glutathionyl spermidine. Subsequently, trypanothione synthetase conjugates another molecule of glutathione to glutathionyl spermidine, forming trypanothione [N1, N8-bis-(glutathionyl)- spermidine]. The synthesized trypanothione is reduced by the enzyme trypanothione reductase (TR) in the presence of NADPH (Comini et al., 2013b). Trypanothione is important for the parasite's survival as it plays a pivotal role in various cellular processes, including the reduction of toxic ROS generated by macrophages and ribonucleotide synthesis (Fairlamb & Cerami, 1992; A. Kumar et al., 2019a). Because of its importance, several enzymes in the trypanothione biosynthesis pathway have emerged as promising drug targets. In vitro and in vivo studies have revealed promising results with natural products, particularly plant-based substances, tested against trypanothione synthetase (UniprotKB: Q9GT49) (PDB id:1VOB) and trypanothione reductase (UniprotKB: P39050) (PDB ID:6ER5) (Polonio, 1998). Additionally, the effects of natural compounds such as conessine, tomatine, uvaol, and botulin on trypanothione synthetase of *Leishmania donovani* have been investigated, demonstrating significant inhibition of the parasite's redox metabolism in invitro studies (Saudagar & Dubey, 2011a). In the present study, our objective is to screen specific inhibitors for glutathione synthetase (GS EC 6.3.2.3) from *Leishmania donovani*. Although glutathione synthetase is also present in the mammalian host, humans possess two isoforms of

glutathione synthetase that show very low sequence similarity (<28%) to *Leishmania donovani* glutathione synthetase. The limited sequence similarity indicates structural differences between the two forms, making it possible to design specific inhibitors against *Leishmania donovani* glutathione synthetase. Hence, inhibiting the glutathione synthetase enzyme may disrupt the trypanothione biosynthesis pathway, ultimately leading to the elimination of the pathogen.

## **3.2 Materials and Methods**

### **3.2.1 Target Preparation**

In the absence of an experimental structure of the Glutathione synthetase of *Leishmania donovani*, we opted for comparative modeling by deriving the amino acid sequence from the UniProt database (Ko et al., 2012; 'UniProt: A Worldwide Hub of Protein Knowledge', 2019) (ID: E9BBX9). The sequence was submitted to the GalaxyTBM server (Ko et al., 2012) for modeling. The GalaxyTBM server performs modeling by generating a reliable core structure using multiple templates followed by alignment of the sequence of both target and template for the final building of a model (Joo et al., 2009; Pei & Grishin, 2014). The final model is further refined by detecting and remodeling unreliable local regions. The crystallographic structure of *Trypanosoma brucei* glutathione synthetase (PDB ID: 2WYO), sharing 42.33% identity, was selected as a template. The model was further submitted to the GalaxyRefine server (Heo et al., 2013) for refinement and validation. The active site of the modeled glutathione synthetase was predicted utilizing the COACH server (Yang et al., 2013), which recognizes the binding site by comparison of complementary binding-specific substructures (TM-SITE) and alignment of sequence profile (S-SITE).

The crystallographic structure of human glutathione synthetase (PDB ID: 2HGS) was obtained from the RCSB PDB database. The crystallographic structures were further checked using PyMOL (Yuan et al., 2017) as described previously in the literature (Kundu & Dubey, 2021) water molecules and ligands were removed.

### 3.2.2 Ligand Library Preparation

The ZINC15 database was chosen for the collection of the raw structures of the ligands. The database contained 1576 FDA approved ZINC compounds which were commercially available. These compounds were further screened to remove any duplicate structures, isoforms, or other inorganic compounds. Finally, 1467 FDA-approved compounds which followed Lipinski's rule of drug-likeness using the FAF drugs4 server (Lagorce et al., 2017; Sterling & Irwin, 2015) were selected. It uses JChem (Csizmadia, 2000) to protonate and prepare biologically relevant tautomers and Omega (Friedrich et al., 2017) for improved three-dimensional conformations for docking. The database was imported into PyRx (Dallakyan & Olson, 2015) and converted to PDBQT format for docking.

### 3.2.3 Molecular Docking

For docking the compounds, PyRx software was utilized, where AutoDock Vina was selected as the docking tool. In the first phase of docking, the model structure of *Leishmania donovani* was imported from the PyRx and converted into pdbqt format. The grid box was centered surrounding the active site by constructing the grid box with dimensions of x  $\frac{1}{4}$  27.995, y  $\frac{1}{4}$  22.826, z  $\frac{1}{4}$  34.958, and a box size of x  $\frac{1}{4}$  25.0, y  $\frac{1}{4}$  25.0, z  $\frac{1}{4}$  25.0. The screening was performed with ten runs for each compound and with an exhaustiveness value of 8. Based on the low binding free energy (kcal/mol),

the top 100 compounds were selected. In the second phase of docking, these selected compounds were screened against the crystallographic structure of human glutathione synthetase. The grid box was set with dimensions of x  $\frac{1}{4}$  44.237, y  $\frac{1}{4}$  5.663, z  $\frac{1}{4}$  19.191, and a box size of x  $\frac{1}{4}$  25.44, y  $\frac{1}{4}$  22.749, z  $\frac{1}{4}$  24.346, based on the active site information. Finally, the top 5 compounds showing the highest differences in binding energy between both these enzymes were selected, and their interactions with *Leishmania donovani* glutathione synthetase were analyzed. UCSF Chimera and LigPlotp (Laskowski & Swindells, 2011) softwares were used to visualize the binding interactions.

### **3.2.4 Molecular Dynamics Simulation Studies**

To access the binding stability of the docked complexes under physiological conditions, molecular dynamics simulations (MDS) were performed for the apo-protein and the top 5 complexes over a duration of 200 ns. GROMACS version 2018, with GROMOS 54a7 force field, was used for conducting the simulations. The ligand parameters were obtained from the ATB server. The SPC water model was utilized to solvate each system within a cubic box measuring 1.2 nm in dimensions. To neutralize the overall charge of the systems, ionization with an accurate concentration of (Na/Cl) was done. The systems then underwent energy minimization so that steric clashes that are present within the systems get reduced. Energy minimization was done using the steepest descent algorithm with a tolerance of 1000 kJ/mol for 50,000 steps.

Following energy minimization, NVT (constant number of particles, volume, and temperature) and NPT (constant number of particles, pressure, and temperature) ensembles were equilibrated. Both ensembles were equilibrated for 500 ps using Berendsen thermostat coupling (Bussi et al., 2007) at a temperature of 300k and

Parrinello-Rahman pressure coupling (Martoňák et al., 2003) at 1.0 bar. The Particle Mesh Ewald (PME) method (Kawata & Nagashima, 2001) was used to compute long-range electrostatic interactions. The LINCS algorithm (Hess et al., 1997) was applied to constrain covalent bond lengths. Subsequently, MD simulations of apoproteins and complexes were run for 200 ns with a time step of 2fs. The generated trajectories were analyzed using GROMACS tools, as described previously in the literature (Pande et al., 2021).

### **3.2.5 MMPBSA Free Energy Analysis**

After generating MD simulation data of all the five complexes, the binding energy contribution by each amino acid residues were calculated. For this purpose, the molecular mechanics/Poisson-Boltzmann surface area (MM/PBSA) method, an efficient and reliable computational tool to determine binding free energies ( $\Delta_{\text{bind}}$ ) between ligands and receptors, was used. For (MM/PBSA) calculation, a set of scripts provided with the `g_mmpbsa` tool (Genheden & Ryde, 2015) was used that employs MD simulation trajectories within the GROMCAS working environment.

## **3.3 Results**

### **3.3.1 Homology Modeling of Glutathione Synthetase**

The structure of *Leishmania donovani* Glutathione synthetase was constructed by homology modeling. The Galaxy server generated five models, among which the model with the lowest MolProbity score (2.303) and a high Ramachandran favored percentage (94.4) was selected as the best model for further study (Figure 3.1). The resultant model consists of 606 amino acids and encompasses 32.0% alpha helix, 2.0% 3–10 helix, 18.2% strand, and 47.9% other structural elements. The predicted

active site residues in the model include 137 R, 175 N, 177I, 178S, 179 C, 180S, 181 F, 289Q, 292E, 294 N, 370 R, 373Y, 581 R, and 597 A. Since in a family of proteins, the conserved amino acid residues have an essential role in stabilizing the protein structure and in catalysis (Sun et al., 2001), we have performed a multiple sequence alignment of the amino acid sequences of Glutathione synthetase of multiple *Leishmania spp* (Figure 3.2). The sequence of the template was also aligned. It was observed that the predicted active site residues are highly conserved among the aligned sequences.

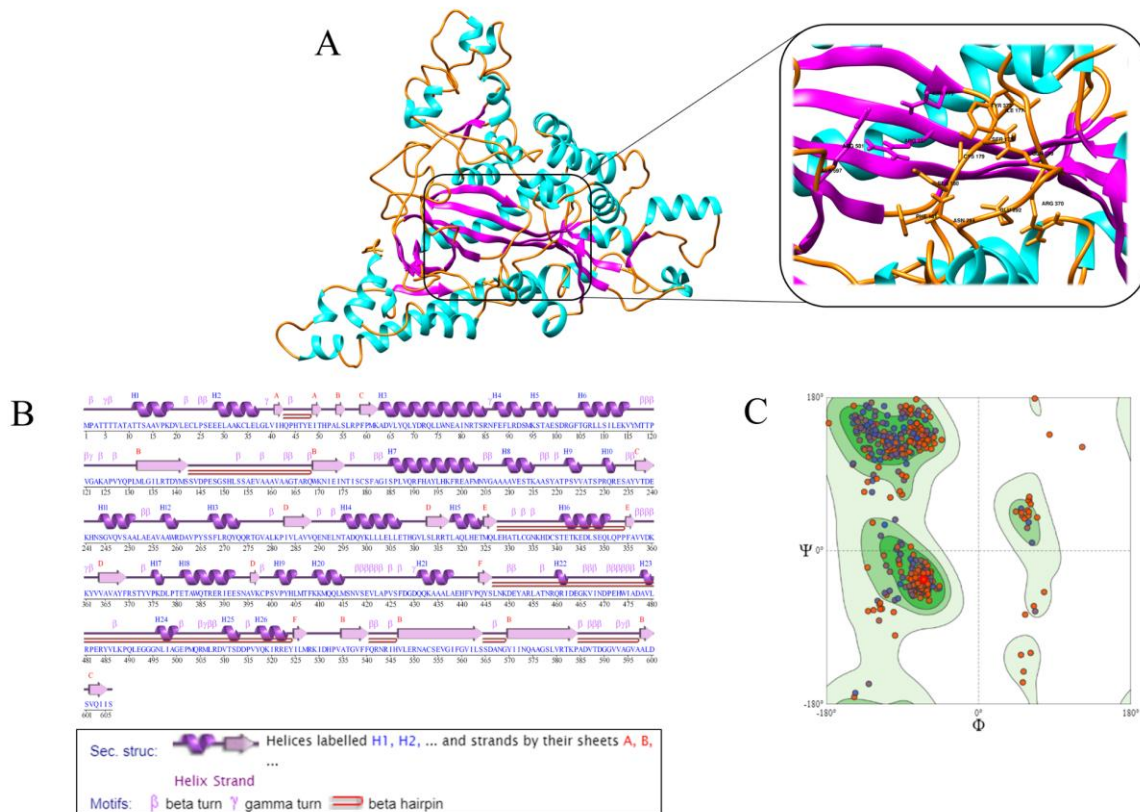


**Figure 3.1: Homology Modeling:** A. Generated model of glutathione synthetase, the predicted active site residues are shown in the inset. B. Secondary structure composition of the model. C. Ramachandran plot.

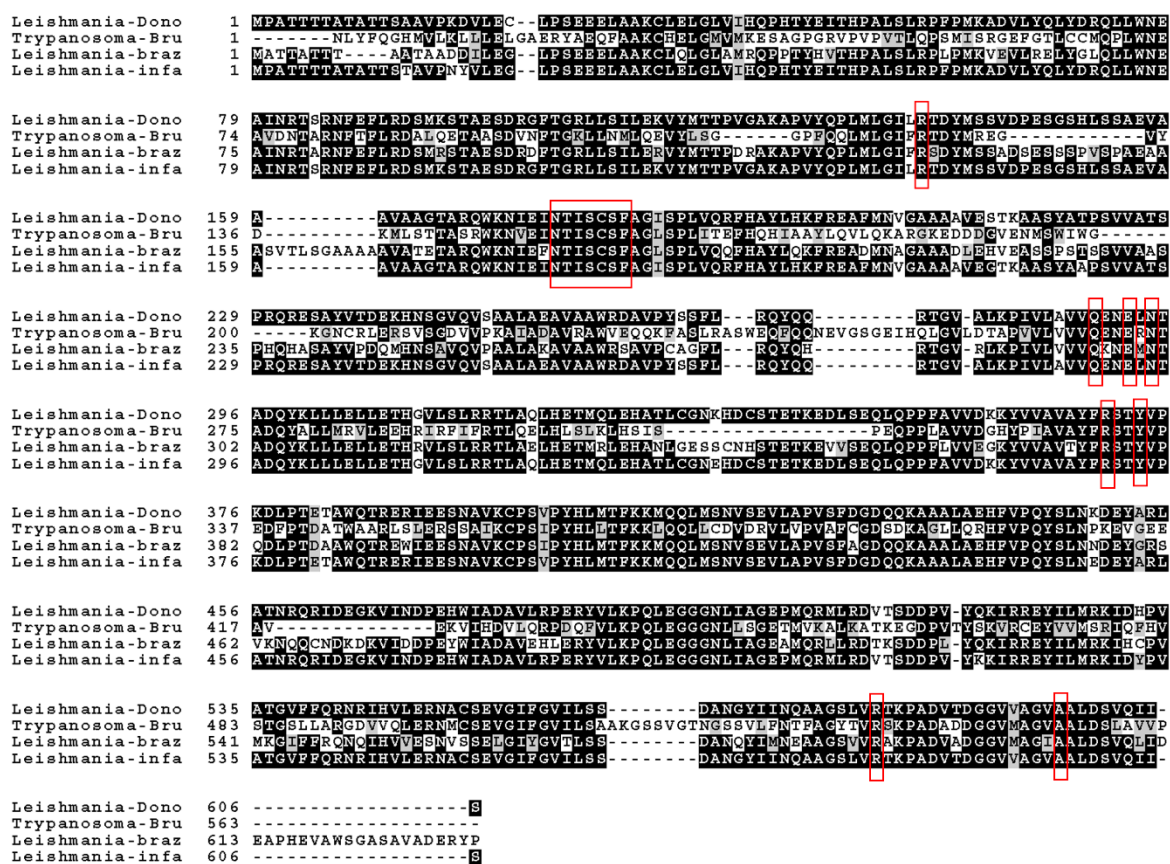
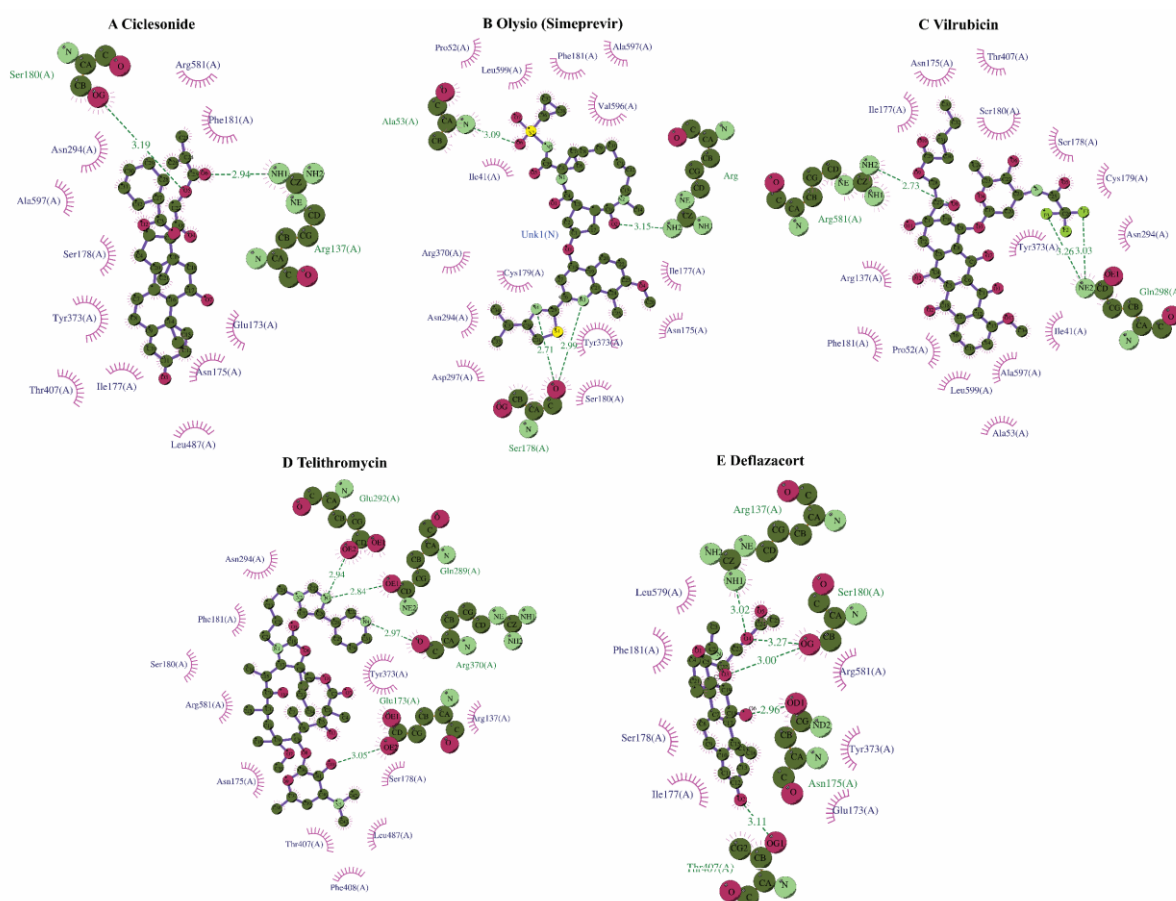


**Figure 3.2: Sequence conservation in Glutathione synthetase:** Multiple sequence alignment of Glutathione synthetase from *L. donovani*, *T. brucei*, *L. braziliensis* and *L. infantum* active-site residues highlighted in boxes.

### 3.3.2 Interactions of the Compounds with *Leishmania donovani* Glutathione Synthetase (LdGS) and Human Glutathione Synthetase (hGS)

Based on the comparative docking analysis of both LdGS and hGS, the compounds having higher affinity towards LdGS were selected (Table 1). Among the chosen compounds, Olysis (ZINC164760756) exhibited the greatest difference (7.3 kcal/mol) in binding affinity with LdGS and hGS. It interacted with LdGS, forming two hydrogen bonds (H-bonds) and 11 hydrophobic interactions with a binding affinity of 9.8 kcal/mol with (Table 2). Similarly, four other compounds were selected based on the differences in binding energy. The compound Valrubicin (ZINC49783788) had a score of 9.2 kcal/mol, followed by Telithromycin (-9.0 kcal/mol), Ciclesonide (-10.1 kcal/mol) and

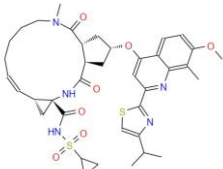
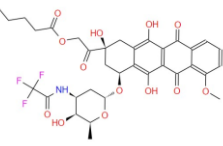
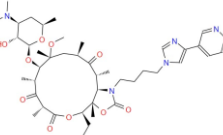
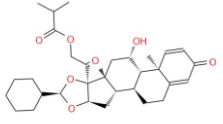
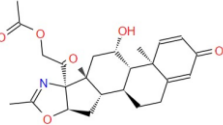
Deflazacort (-9.2 kcal/mol). The overall binding energy of all the compounds ranged from 9.0 kcal/mol to 10.1 kcal/mol. Significant contributions to the interaction between protein and ligand were due to critical hydrogen bonds and hydrophobic interactions. Residues such as Arg137, Asn175, Ile177, Ser178, 180, Cys179, Asn294, Gln298, Asp297, Tyr373, and Arg581 played a critical role in fundamental interactions forming both hydrogen and hydrophobic bonds (Figure 3.3). The fundamental interactions and binding energies of all these compounds are represented in Table 2.1.



**Figure 3.3: LIGPLOT images:** Visualizing the docked protein-ligand complexes. Ligand atoms are depicted as smaller spheres with purple intramolecular bonds, while amino acid atoms are represented as comparatively larger spheres. Dashed green lines, along with distance represent

the hydrogen bonds and magenta arcs represent the amino acid residues forming hydrophobic interactions

**Table 3.1:** Binding affinity comparison between *L. donovani* glutathione synthetase and human glutathione synthetase

SI No	Ligand ID	PubChem CID	Ligand name	Binding Affinity with model <i>LdGS</i> (kcal/mol)	Binding Affinity with hGS (kcal/mol)	Difference In binding energies
1	ZINC00016476075 6 	24873435	Olysio	-9.8	-2.5	7.3
2	ZINC00004978378 8 	454216	Valrubicin	-9.2	-2.4	6.8
3	ZINC00000957477 0 	3002190	Telithromycin	-9	-3.2	5.8
4	ZINC00000391515 4 	6918155	Ciclesonide	-10.1	-4.9	5.2
5	ZINC00000421280 9 	189821	Deflazacort	-9.2	-4.4	4.8

**Table 3.2: Results of the interactions of docked complexes**, emphasizing binding energy, hydrogen, and hydrophobic interactions, numbers in parentheses include the length of hydrogen bonds

SL No.	Compound ID	Name	Binding Affinity (kcal/mol)	Amino acid residues forming H-bonds (Length in Å)	Amino acid residues forming Hydrophobic Interactions
1	ZINC000164760756	Olysio	-9.8	Ala53(3.09) Ser178(2.71), Arg581(3.15),	Ilu41, Pro52, Asn175, Ilu177, Cys179, Ser180, Phe181, Asn294, Asp297, Arg370, Tyr373, Val596 Ala597, Leu599
2	ZINC000049783788	Valrubicin	-9.2	Gln298 (3.03, 3.26) Arg581(2.73)	Ile41, Pro52 Ala53, Asn175, Ile177, Ser178, Cys179, Ser180, Phe181, Asp294, Tyr368, Tyr373, Thr407, Ala597, Leu599
3	ZINC000009574770	Telithromycin	-9	Glu173(3.05), Gln289(2.84) Glu292(2.94) Arg370(2.97)	Arg137, Asn175, Ser178, Ser180, Phe181, Asn294, Tyr373, Thr407, Phe408, Leu487, Arg581
4	ZINC000003915154	Ciclesonide	-10.1	Arg137(2.94), Ser180(3.19)	Glu173, Asn175, Ile177, Ser178, Phe181, Asn294, Tyr373, Thr407, Leu487, Arg581, Ala597,
5	ZINC000004212809	Deflazacort	-9.2	Arg137(3.02), Asn175(2.96), Ser180(3.27), Thr407(3.11)	Arg58, Glu173, Ile177, Ser178, Phe181, Tyr373, Leu579

### 3.3.3 Dynamics of Protein-Ligand Complexes

After conducting molecular dynamic (MD) simulation of the apoprotein and all the five complexes for 200 ns, the generated trajectories were assessed to understand the stability of the protein-ligand interactions. The evaluation was done by analyzing the trajectories of Root Mean Square Deviation (RMSD) of the protein's backbone, Radius of Gyration (Rg), and intramolecular hydrogen bonds formed. The RMSD trajectory of Ciclesonide, Olysio, and Telithromycin complexes displayed a similar pattern to that of the apoprotein, and with an average RMSD rise of 0.6 nm. Similarly, the complex from Valrubicin had an average RMSD of 0.5 nm [Figure 3.3 (A)]. However, the complex formed by Deflazacort exhibited an upward RMSD trajectory after approximately 150 ns. To evaluate the compactness of the protein structure, Rg plots were analyzed. The apo-protein and the complexes formed by Ciclesonide and Telithromycin exhibited a similar Rg pattern, with an average value of around 2.65 nm. The Olysio and Valrubicin complexes displayed a slightly higher Rg value of 2.7 nm on average. Interestingly, the complex formed by Deflazacort initially displayed a lower Rg value of approximately 2.63 nm until 130 ns after which it displayed an upward trajectory that rose to 2.7 nm [Figure 3.3 (B)]. The formation of intermolecular hydrogen bonds plays a crucial role in the overall stability of the protein-ligand complexes. The analysis revealed the average number of hydrogen bonds formed throughout the 200 ns simulation period for all five complexes [Figure 3.3 (C)]. The complex formed by Valrubicin had 7 hydrogen bonds, followed by the complex of Olysio which had 6 hydrogen bonds on an average. The complex Telithromycin had 3 hydrogen bonds on an average, whereas Ciclesonide and Deflazacort both formed 2 hydrogen bonds on an average. This analysis provides insights into the overall stability of the protein-ligand complexes. A similar pattern in the RMSD of the apoprotein and certain

complexes indicated a relatively stable binding, while the rise of the RMSD trajectory from by the complex Deflazacort after 150 ns suggests potential conformational changes or fluctuations. The Rg values with slight variations further support the compactness of the protein-ligand complexes. The number of hydrogen bonds formed provides a quantitative information about the strength and number of interactions between the protein and the ligands. Overall, these results suggested that the complexes are stable upon ligand binding. The complex formed by Deflazacort has comparatively lower stability, where higher RMSD and Rg values and fewer intermolecular hydrogen bonds were observed.

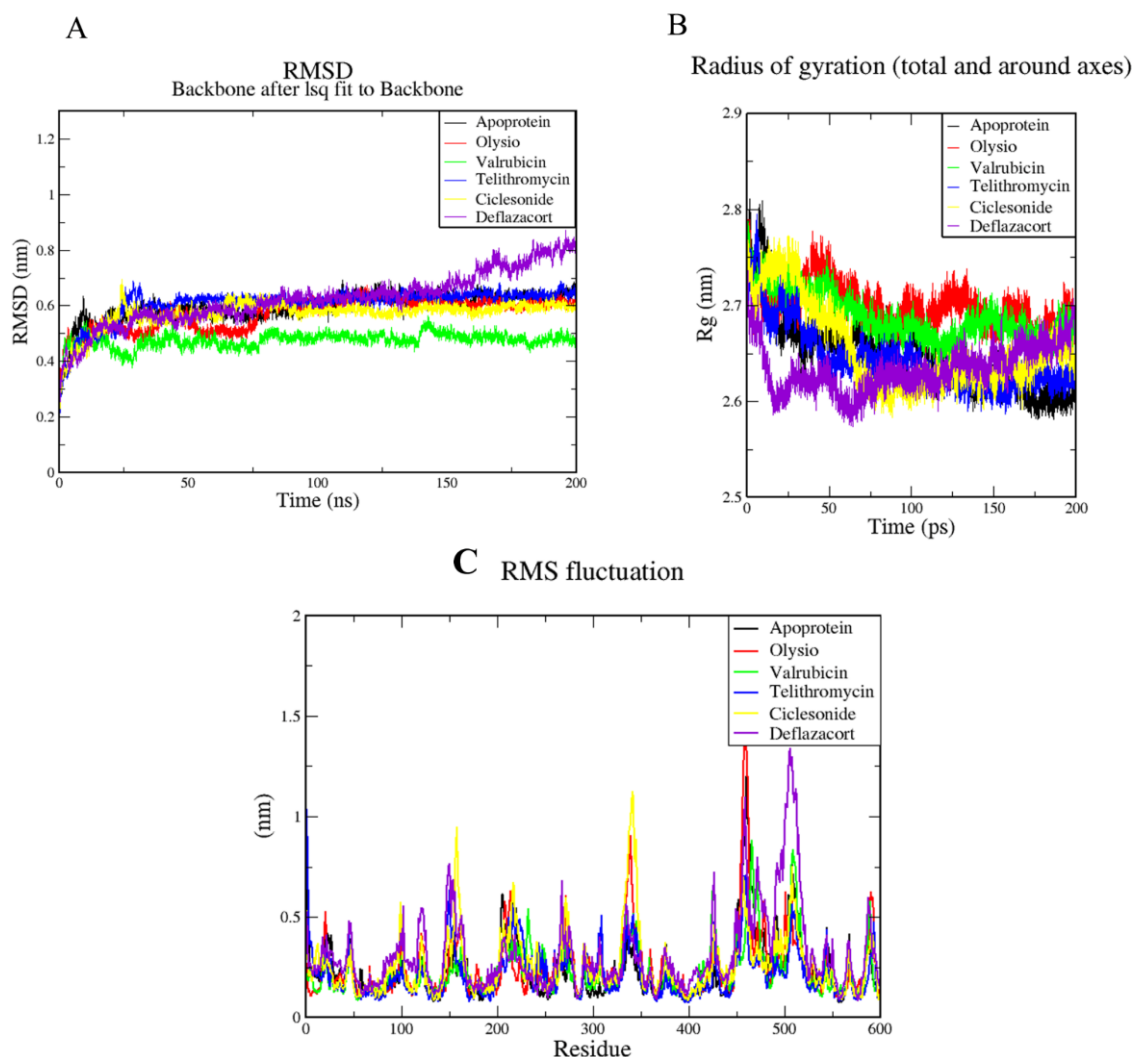


**Figure 3.4:** Analysis of simulated trajectories: A) Root Mean Square Deviation (RMSD) of the protein's backbone: Illustrates the stability and conformational changes of the protein backbone throughout the simulation, B) Radius of gyration (Rg): Shows the compactness or size of the protein during simulation.

### 3.3.4 Binding Free Energy Calculation

For a further investigation of protein-ligand interaction, we conducted post simulation binding free energy analysis. This analysis was done using the final 50 ns trajectory obtained from the Molecular Dynamic (MD) production run. We selected 250 snapshots for protein-ligand complex at an interval of 0.2 ns to have a comprehensive representation of the binding dynamics. Among the five complexes, Olysio had the lowest binding free energy with a value of 89.21

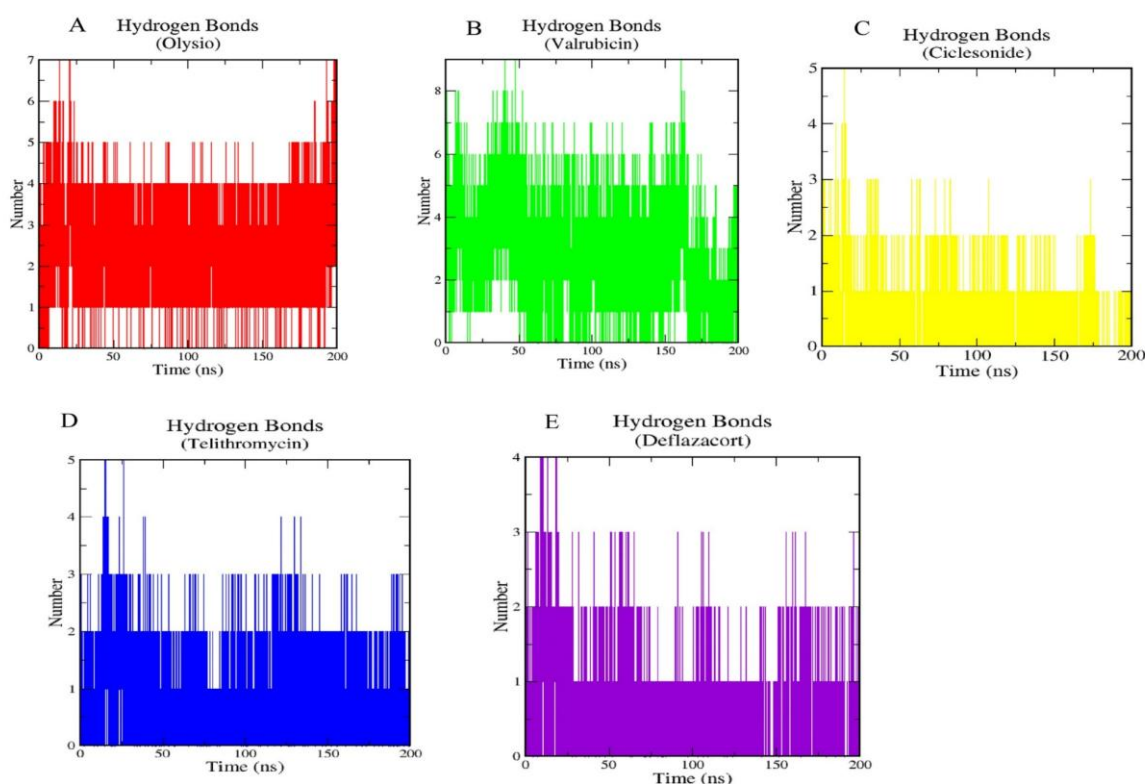


**Figure 3.5: Analysis of hydrogen Bond formation in the protein-ligand complexes:** the figure illustrates the number of hydrogen bonds formed between the protein and the ligands throughout the 200 ns simulation. A. Olysio, B. Valrubicin, C. Ciclesonide, D. Telithromycin, and E. Deflazacort.

kcal/mol. Telithromycin and Valrubicin followed with the binding free energies of 45.34 kcal/mol and 37.04 kcal/mol, respectively. The other two complexes, Ciclesonide (-22.11 kcal/mol), and Deflazacort (-19.47 kcal/mol) displayed comparatively lower binding free energies (Table 3). In the case of Olysio, the Van der Waals energy, electrostatic energy, and polar solvation energy contributed significantly to the overall binding energy. Whereas for the other four complexes, the Van der Waals energy and polar solvation energy played a significant role. The specific nature of these interactions varied with the different ligands indicating their different molecular properties and modes of interaction with the active site of the protein.

**Table 3.3:** MM/PBSA binding free energy analysis of all the protein-ligand complexes

Complex	Binding Energy (kcal/mol)	Van der Waals Energy (kcal/mol)	Electrostatic Energy (kcal/mol)	Polar Solvation Energy (kcal/mol)	SASA Energy (kcal/mol)
Olysio	-89.21 ± 9.36	-77.25 ± 8.84	-78.03 ± 6.55	74.47 ± 7.9	-8.4 ± 0.57
Telithromycin	-45.34 ± 4.42	-70.23 ± 3.96	-8.78 ± 2.53	40.39 ± 5.25	-6.72 ± 0.4
Valrubicin	-37.04 ± 4.62	-67.98 ± 5.99	-9.14 ± 3.47	47.61 ± 6.55	-7.54 ± 0.36
Ciclesonide	-22.11 ± 0.42	-44.14 ± 0.56	-4.06 ± 0.12	31.23 ± 0.46	-5.17 ± 0.06
Deflazacort	-19.47 ± 14.96	-36.45 ± 17.76	-2.42 ± 1.92	23.48 ± 11.08	-4.08 ± 1.99

### 3.4 Discussion

Visceral Leishmaniasis (VL) exhibits a significant public health concern, particularly in developing countries like India and Africa, associated with risk factors such as poverty,

malnutrition, migration, and environmental changes contributing to the increased susceptibility to the disease. VL has a high fatality rate if left untreated, exceeding 95%. The current treatment approach depends primarily on multidrug therapy consisting of Miltefosine, Amphotericin B, and Paromomycin sulfate, which has shown considerable effectiveness with a cure rate of approximately 97% (Sundar & Chakravarty, 2015; Thakur et al., 2001). However, there have been reports of new VL cases in non-endemic regions of India in recent decades (Dhiman, 2014; Khanra et al., 2012). The complete elimination of the disease is facing challenges due to the lack of a vaccine, inadequate vector control measures, high cost of available drugs, and lengthy treatment duration. Additionally, the emergence of drug-resistant strains of the *Leishmania* parasite further complicates the situation (Krayter et al., 2014). Because of these challenges, the development of new therapeutic strategies is essential to discover a drug with high efficacy and minimal side effects for VL treatment.

We have achieved significant progress in identifying inhibitors for the glutathione synthetase enzyme of *Leishmania donovani*. By targeting this enzyme, we can effectively disrupt the redox metabolism of the parasite. *Leishmania* parasites are known to be highly sensitive to oxidative stress, making the inhibition of their redox metabolism an effective strategy for eliminating the parasite. The alignment confirmed that the enzyme is indeed conserved within the parasite. Based on this observation, we anticipate that drugs inhibiting the glutathione synthetase enzyme will be particularly effective against drug-resistant strains of the parasite.

In our study, we screened a large number of FDA-approved drugs that follow Lipinski's rule of drug-likeness to ensure that the selected drugs would be suitable for oral administration and have minimal side effects. By molecular docking studies, we identified five drug candidates that exhibited a high binding affinity with the active site

of the enzyme. To further evaluate the stability of these drug candidates, we performed molecular dynamics (MD) simulations for 200 ns. Analyzing the parameters of RMSD, Rg, and hydrogen bonds, we obtained valuable insights into the stability of the drug candidates when bound to the enzyme's active site. Among the five drug candidates, namely Olysio (Simeprevir), Telithromycin, Valrubicin, Ciclesonide, and Deflazacort, four of them, namely Olysio, Telithromycin, Valrubicin, and Ciclesonide demonstrated good stability upon binding to the active site of the enzyme. However, the drug candidate Deflazacort showed slightly lower stability in comparison. Further evaluation of the binding strength of these drug candidates, we performed post simulation free energy analysis. This analysis revealed that the drug Olysio has the lowest binding free energy, indicating a strong and favorable binding free energy. Telithromycin followed closely with a second most favorable binding free energy.

Among the five drug candidates identified, Olysio, Telithromycin, Valrubicin, and Ciclesonide showed promising stability, making them strong candidates for further experimental study as anti-leishmanial drugs. Olysio, also known as Simeprevir is used for chronic hepatitis C virus (HCV) infection in adults inhibiting NS3/4A protease of hepatitis C virus (HCV) (Raboisson et al., 2008). The common side effects reported with the use of Olysio is to have nausea, itching and skin rash. Telithromycin, a synthetic erythromycin derivative, is used to cure community-acquired pneumonia (Bearden et al., 2001) and acts by blocking protein synthesis. Telithromycin is reported to have mild to moderate side effects such as gastrointestinal disturbances, headache etc. Valrubicin, an anthracycline chemotherapy drug functions by damaging DNA extensively and by interfering the function of DNA topoisomerase-II and thus arresting cell cycle in G2 (Onrust & Lamb, 1999a). Being a chemotherapy drug, Valrubicin is reported to have more significant side effects, like bone marrow suppression, hair loss,

gastrointestinal issues etc. But the use of Valrubicin as an anti-leishmanial drug might involve lower doses and potentially reduce the risk of side effects. Ciclesonide, a glucocorticoid used to treat obstructive airway diseases. The mechanism of the action of Ciclesonide has been shown by inhibiting leucocyte infiltration at the site of inflammation and suppressing humoral immune response (Mutch et al., 2007). Being a glucocorticoid drug, Ciclesonide may have local side effects like throat irritation. The fifth drug, Deflazacort also known as Emflaza is used to treat children with Duchenne muscular dystrophy (DMD)(BIGGAR, 2004). Like other corticosteroid, Deflazacort may have side effects like weight gain, increased appetite etc. Based on their known properties and mechanism of action, these drugs can also exhibit anti-protozoal activity. In conclusion, our study has successfully identified five drugs as potential inhibitors of the *Leishmania donovani* glutathione synthetase enzyme. By targeting this enzyme and inhibiting the redox metabolism of the parasite, we can effectively combat drug-resistant strains of *Leishmania*. In our previous work we have validated the computational inhibitor design using experimental studies on other drug targets (Saudagar & Dubey, 2014a;O. P. Singh et al., 2016). However, the study requires further in vitro experimental studies as well as clinical validations of these inhibitors to ultimately provide a novel strategy to control the disease.